# Synthesis and Optical Properties of Cu2CoSnS4 Colloidal Quantum Dots

Arnaud Gillorin, Andréa Balocchi, Xavier Marie, Pascal Dufour, Jean-Yves Chane-Ching

# Synthesis and Optical Properties of $Cu_2CoSnS_4$ Colloidal Quantum Dots

**A. Gillorin,[a] A. Balocchi,[b] X. Marie,[b] P. Dufour[a] and J. Y. Chane-Ching*[a]**

Monodisperse quaternary chalcopyrite $Cu_2CoSnS_4$ colloidal quantum dots have been synthesized by acid peptization of a tailored $Cu_2CoSnS_4$ precursor displaying loosely packed, ultrafine primary crystallites. Well-defined peaks shifted to higher energy compared to the $Cu_2CoSnS_4$ bulk band gap value were observed on the UV-Vis absorption curve consistent with a quantum confinement behavior. First investigations by room temperature time resolved photoluminescence (TRPL) spectroscopy suggest that the photoluminescence emission does not arise from a donor–acceptor recombination.

## Introduction

Chalcopyrite semiconductors have attracted intense interest within the past 25 years owing to their appropriate band gap ($CuInS_2$, CIS, 1.5 eV, $CuInSe_2$ 1.1 eV) well matching the AM0 solar spectrum.[1,2] High efficiencies close to 20% have been achieved on solar cells based on these materials. Recently,[3,4] the quaternary chalcopyrite compound $Cu_2ZnSnS_4$ (CZTS) which contains only abundant and non-toxic elements has become the subject of intense interest because it is an ideal absorber candidate material for thin film solar cells[5] with an optimal band gap (1.5 eV) and high absorption coefficient ($>10^4$ $cm^{-1}$). The reported energy conversion efficiency of CZTS-based solar cells has increased from 0.66% to close to 10% very recently.[4] CZTS possess a crystal structure which is analogous to the chalcopyrite type semiconductors such as $CuInGaS_2$ and belongs to an entire class of quaternary materials including $Cu_2ZnSnS_4$, $Cu_2CoSnS_4$, $Cu_2FeSnS_4$.[6] To improve its performance, new design concepts have been implemented increasing these materials' efficiencies to values exceeding that of single gap solar cells. Intermediate band solar cells[7] were recently proposed consisting in the introduction of impurity levels in the middle of the semiconductor band gap allowing for the absorption of additional lower energy photons. In this context, quantum dot (QD) arrays provide the intermediate band of discrete states that allow sub-band gap energies to be absorbed. Chalcopyrite QDs were reported as promising materials for photovoltaic devices since they offer many advantages such as high absorption coefficient, structural defect tolerance, insensitivity to radiation damages.[8] Thus, chalcopyrite QDs have been proposed as candidates for Si-based intermediate band solar devices.[9] However, only a few reports[10,11] concerning the synthesis of quaternary chalcopyrite nanocrystals have been published to date. CZTS nanocrystals were for instance synthesized by high temperature-arrested precipitation in the coordinating solvent oleyamine (OLA). The particles are crystalline and have an average diameter of 10 nm or 15–20 nm with band gap energy, determined from the absorbance spectra, respectively of 1.3 eV and 1.5 eV suggesting no quantum confinement effects for the synthesized nanocrystals.[10,11] In addition, to further improve the efficiency of the quaternary chalcopyrite QD-based solar cells, it is crucial to understand the optical properties of these building blocks. Indeed, only a few reports[12–14] describe the optical properties of quaternary chalcopyrites. These investigations have only dealt with CZTS bulk materials such as thin film prepared by sol-gel and sulfurization method, as well as bulk single crystal.

Here, we report on a novel approach to the synthesis of monodisperse chalcopyrite $Cu_2CoSnS_4$ semiconductors QDs. $Cu_2CoSnS_4$ QDs were synthesized without the use of any high selectivity coordinating ligand or coordinating solvent. Our process route includes, in a first step, the preparation of a precursor displaying a unique $Cu_2CoSnS_4$ structure and possessing low primary crystallite size, loosely packed. In a second step, the formation of $Cu_2CoSnS_4$ quantum dots was achieved by acid peptisation. Absorption spectra collected on $Cu_2CoSnS_4$ QDs dispersions synthesized without coordinating surface species clearly displays two well-resolved peaks in the UV-visible spectral region. Optical properties of these quantum dots were fully investigated by stationary (PL) and time resolved (TRPL) photoluminescence spectroscopy.

## Experimental section

### Preparation of $Cu_2CoSnS_4$ Precursor

A typical procedure of $Cu_2CoSnS_4$ precursor synthesis follows 9 mmol of $CuCl_2 \cdot 2H_2O$, 4.5 mmol of $CoCl_2 \cdot 6H_2O$, 4.5 mmol of $SnCl_4 \cdot 5H_2O$ and 180 mL of absolute ethanol mixed at room temperature. Once the metal salts were completely dissolved, 45 mmol $CS(NH_2)_2$ were added, then 3.85 mL of TMaOH 25% in

[a]*CIRIMAT, CNRS, INPT, Université de Toulouse, 118, Route de Narbonne, 31062 Toulouse, Cedex 9, France. E-mail: chane@chimie.ups-tlse.fr*
[b]*LPCNO, INSA, CNRS, Université de Toulouse, 135, Avenue de Rangueil, 31077 Toulouse, Cedex 9, France*

DOI: 10.1039/c0jm03964k

MeOH were injected. After 10 mn, 9 mmol of ascorbic acid were incorporated into the reaction mixture which was adjusted to 240 mL with ethanol. The resulting mixture was transferred into a Teflon-lined stainless steel autoclave with a capacity of 600 mL and heated at 200 °C and maintained for 16 h. After cooling, the suspension was centrifuged at 3500 rpm resulting in a solid pellet P and a supernatant which was eliminated. For the characterization of the precursor, the solid pellet was washed with ethanol and dried at room temperature.

### Preparation of $Cu_2CoSnS_4$ Quantum Dots by Peptisation

The solid pellet P previously described was directly re-dispersed after centrifugation at room temperature in an ethanol solution containing 2 M acetic acid. Peptisation was performed by keeping the suspension under continuous stirring for about 16 h at room temperature. Size selective precipitation was achieved by centrifugation at 3500 rpm. The colloidal sol obtained was further subjected to acetic acid removal involving precipitation of solid by hexane addition, centrifugation and re-dispersion in ethanol. Orange-red colloidal $Cu_2CoSnS_4$ quantum dots dispersions in ethanol were thus obtained after several washing steps.

### Measurements

Elemental analysis (ICP-OES) was performed by Service Central d'analyses, CNRS, Solaize, France. High resolution transmission electron microscopy (HRTEM) images were taken using a JEOL 1011 operating at 100 kV in bright field mode. A LabRAM HR 800, Jobin Yvon Raman spectrometer was used to record Raman spectra. The spectral resolution of the monochromator was about 1 $cm^{-1}$. For optimum signal-to-noise ratio, we selected the red line of the He–Ne laser with an excitation wavelength $\lambda = 632.82$ nm and an excitation power $P_{He-Ne} = 1.7$ mW.

Optical absorption spectra were recorded on a VARIAN Carry 10 spectrophotometer. Cuvettes used for the experiments are made of Suprasil quartz from Hellma Analytics. In order to avoid artifacts, the cuvettes contribution to the absorption has been systematically subtracted from the raw data. Continuous wave photoluminescence spectra were recorded on a Acton Spectra Pro 2500 I spectrofluorometer equipped with an $Ar^+$ ion laser ($\lambda = 351$ nm, Newport Beam lock Ae 2065-7S) or a GaN diode laser ($\lambda = 405$ nm, Nichia NLHV 3000E). Measurements were performed on nanocrystals solutions, placed in 1-cm quartz cuvettes. Time-resolved photoluminescence was performed using a frequency-tripled mode-locked Ti-saph laser with 1.2 ps pulse duration and 80 MHz repetition frequency, at a wavelength $\lambda =$ 290 nm and average power $P_{aver} = 1$–10 mW, focussed to a 50 μm diameter spot. The PL dynamics is recorded with a S20 photocathode Hamamatsu synchroscan Steak Camera C5680 with 8 ps overall time resolution.

## Results and discussion

### $Cu_2CoSnS_4$ Precursors

$Cu_2CoSnS_4$ nano-crystals were prepared from a surfactant-free route using solvothermal synthesis. Our process involves in a first step, the preparation of a $Cu_2CoSnS_4$ precursor possessing loosely packed ultrafine primary crystallites. Formation domains of samples exhibiting a unique $Cu_2CoSnS_4$ structure by XRD (Fig. 1) were investigated by variation of [S]/[Cu] and [OH]/[Cu] where [S] denotes for the total concentration of sulfur species in the reaction solution and [OH] for the base concentration. $Cu_2CoSnS_4$ formation domain was investigated in the range of OH/Cu ratios corresponding to the partial neutralization of the metallic cations. Formation of a unique ternary chalcopyrite $Cu_2CoSnS_4$ structure is observed in a large domain. It is worth noting that, for reaction mixtures prepared at higher OH/Cu ratios, formation of the $Cu_2CoSnS_4$ structure is only achieved in high-sulfide concentration medium. Alternately, highly super-saturated conditions were classically defined by variation of reaction temperature and duration. A crucial parameter for adjusting the super-saturation is the ascorbic acid addition which increases [$Cu^+$], resulting in a significant decrease of $Cu_2CoSnS_4$ XRD domain size. In ethanol as solvent, a loose packing of the primary crystallites was achieved through a fine tuning of [OH] concentration. Thus, typical conditions for preparation of precursor displaying a unique $Cu_2CoSnS_4$ structure with ultrafine primary crystallites, loosely packed was (Cu : Co : Sn : S : OH) = (2.0 : 1.0 : 1.0 : 10 : 2). Synthesis at 200 °C for 16 h yields primary crystallite size, calculated using Scherrer's equation on (112) XRD peak, of 6 nm. This primary crystallite size value was confirmed by high resolution TEM images recorded of this sample showing particles formed by aggregation of primary crystallite of 3–6 nm. Typical chemical composition of the precursor determined by chemical analysis shows a Co deficient composition (Cu : Co : Sn : S) = (2.0 : 0.77 : 0.96 : 3.91). A Raman investigation was undertaken to understand deviations from stoichiometry. As a reference, a highly crystalline $Cu_2CoSnS_4$ sample was synthesized following a procedure previously described.[15] The high temperature sample synthesized at 500 °C displays a main peak at 327 $cm^{-1}$ and secondary peaks observed at 302 $cm^{-1}$ and 350 $cm^{-1}$. Compared

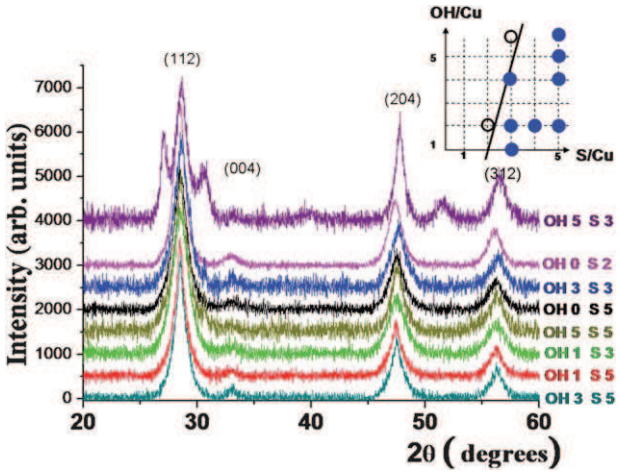


**Fig. 1** XRD patterns of $Cu_2CoSnS_4$ precursors. The XRD pattern of a sample synthesized at [OH]/[Cu] = x and [S]/[Cu] = y is referenced OHx Sy. (The curves have been vertically displaced for clarity.) Inset: formation domain of $Cu_2CoSnS_4$ structure in the [OH]/[Cu], [S]/[Cu] diagram. Black dots represent conditions of formation of a unique $Cu_2CoSnS_4$ structure revealed by XRD. Diffraction planes of $Cu_2CoSnS_4$ are reported (Reference JCDD-No 26-0513).

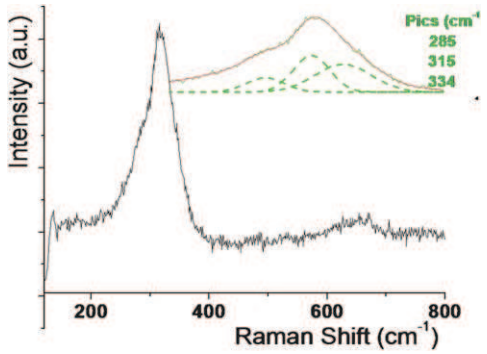


**Fig. 2** Typical Raman spectrum of $Cu_2CoSnS_4$ precursor. Inset: deconvolution of the 200–400 nm broad peak.

with values reported in the literature for $Cu_2ZnSnS_4$ and $Cu_2FeSnS_4$,[16] our assignments for $Cu_2CoSnS_4$ are consistent with the previous findings of Koschell *et al.*[17] Indeed, they predicted that in the closely related chalcopyrites the totally symmetric vibration is found near 300 $cm^{-1}$ and hardly varies since it is a motion of the sulfur atoms alone. Raman spectra recorded on $Cu_2CoSnS_4$ precursor samples (Fig. 2) consist of a broad peak located in the range of 200–400 $cm^{-1}$. Three peaks, shifted at lower energies (285 $cm^{-1}$, 315 $cm^{-1}$ and 337 $cm^{-1}$) were observed after de-convolution of this broad peak. Since small variations in frequencies were observed for these three lines compared with those determined on bulk samples, further investigation is under progress to better define contributions of parameters such as quantum confinement or deviations to stoichiometric composition to account for the origin of the observed small variations in peak energy of our nano-crystallites. We can conclude from all these observations that the formation of a $Cu_2CoSnS_4$ precursor with small deviations from stoichiometric composition can be ascribed to the presence of some amorphous phase.

### $Cu_2CoSnS_4$ Quantum Dots

Electrostatic stabilization by acid peptization[18,19] is largely employed for the fabrication of colloidal nanocrystals. The colloidal dispersions we prepared at 1 g $L^{-1}$ were shown to be stable towards decantation for more than 6 months.

HRTEM observation shows a fairly monodispersed population of nanoparticles without significant aggregation (Fig. 3). Fine inspection of the TEM images indicates particles displaying a spherical morphology with an average diameter of $3 \pm 1$ nm. A similar composition (Cu : Co : Sn : S) = (2.00 : 0.69 : 0.90 : 3.42) compared to those determined for the precursor was established by chemical analysis of the colloidal dispersion although some samples may exhibit a more deficient copper composition. Because of the ultra-thin size of the nanoparticles, chemical heterogeneities were investigated using EDS-TEM performed with a local probe as small as 5 nm. All our investigations did not show a measurable presence of $SnS_2$, CoS or $Cu_xS$ nanocrystals.

### Optical Properties of $Cu_2CoSnS_4$ Quantum Dots

Optical properties of the nano-crystals were investigated using room temperature photoluminescence and UV-Vis-NIR

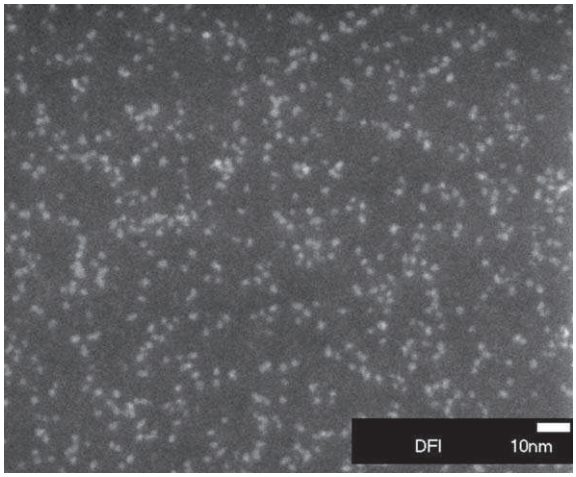


**Fig. 3** HRTEM image of $Cu_2CoSnS_4$ quantum dots showing a monodisperse population of 3 nm discrete nanoparticles.

absorption spectroscopy. The absorption spectrum (Fig. 4) recorded on the $Cu_2CoSnS_4$ nano-crystal dispersions shows two well-resolved peaks, observed at 400 nm (3.10 eV) and 480 nm (2.58 eV). The room temperature photoluminescence spectra recorded on the same dispersions are also plotted and exhibit, as well, two well-resolved peaks at 430 nm (2.88 eV) and 560 nm (2.21 eV). It is worth noting that those two peaks are observed using two different excitation wavelengths (351 nm and 290 nm) in the UV range.

In contrast to CdS[20] or InP[21] semiconductor QDs, numerous studies performed on chalcopyrite QDs (CIS) invariably show a lack of a distinct exciton peak in the absorption spectrum.[22–25] The absorption spectra of the CIS dispersions exhibited a broad shoulder with a long tail to lower energies both significantly shifted from the bulk band gap absorption of CIS. Several factors were proposed to account for this undistinguishable peak such as a more important composition variation for ternary compounds, a very large size distribution, an electron density leakage from the core of the nanocrystals into the organic ligand surface layer, or the presence of intraband states (defect states).

Absorption spectra recorded on our $Cu_2CoSnS_4$ nanocrystal dispersions, composed of nanocrystals possessing

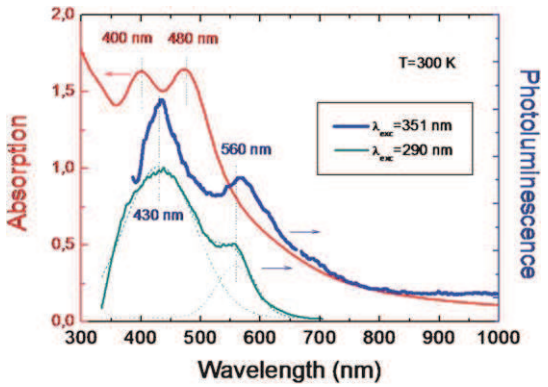


**Fig. 4** UV-Vis-NIR absorption and PL spectra of the $Cu_2CoSnS_4$ quantum dots obtained by peptisation of the precursor prepared from a surfactant-free route. Dotted lines are Gaussian fits of the PL peaks.

a monodisperse size distribution and non-capping surfaces clearly exhibit distinct exciton peaks. Fig. 5 demonstrates that these peaks cannot be ascribed to soluble species formed from the reaction solution. Indeed, spectra recorded on the supernatant of the reaction solution after precursor solvothermal synthesis did not show the two distinct peaks. Since these well-defined peaks on the absorption spectra were observed on $Cu_2CoSnS_4$ colloids whose precursors were synthesized at a relatively low temperature $T = 200$ °C, we anticipate the presence of a large concentration of defects in our nanocrystals, yielding intraband states. However, as shown by our results, the presence of intraband states is not critical to the observation of these distinct peaks in the absorption spectra.

For reference, the bulk band gap energy of $Cu_2CoSnS_4$ was determined on a highly crystalline $Cu_2CoSnS_4$ that we synthesized following a previously described procedure.[15] A value $E_{gap} = 1.5$ eV similar to the bulk band gap of a closely related material $Cu_2ZnSnS_4$ was obtained. Hence, compared with the bulk band gap value, we observed for the $Cu_2CoSnS_4$ nanocrystals a significant blue shift in the peak energies of the UV-Vis absorption spectra. This shift of the absorption peaks energy to higher values is consistent with a quantum confinement effect.

PL spectra exhibited two well-defined peaks, observed at lower energies than absorption peaks with shift values varying from 30 to 80 nm. With the objective of better understanding the transitions involved in these peaks, the PL excitation power dependence was investigated on the $Cu_2CoSnS_4$ QDs (not shown). No significant modification of the spectra was observed in the power range from 1 to 10 mW. Indeed, an alternative interpretation consists in assigning the two PL peaks to the radiative recombination of the ground and excited state in a given size and composition QD.[26] We rule out this interpretation since we do not observe any variation of the relative intensity of the two peaks when the excitation intensity increases. Thus, we believe that these two peaks do not involve transitions occurring in the same chemical compound but it rather suggests transitions occurring either from two populations possessing different mean sizes or from different chemical compounds. Note that two different chemical compounds can develop a same size or be coupled in a core-shell type structure.

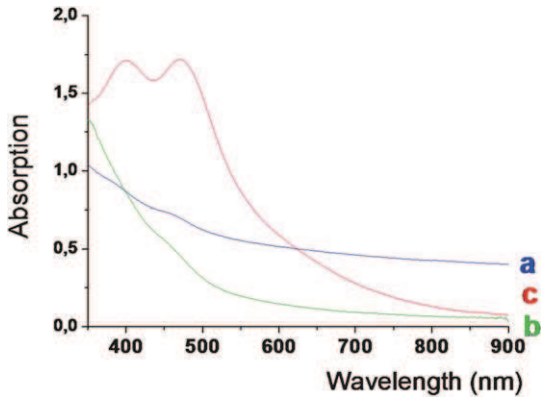


**Fig. 5** UV-Vis absorption spectra of (a) reaction solution after solvothermal synthesis; (b) supernatant obtained by centrifugation of the reaction solution after solvothermal reaction; (c) $Cu_2CoSnS_4$ quantum dots colloidal dispersion.

Because the TEM examination shows a fairly monodisperse size distribution, we can conclude that these two peaks probably arise from the presence of two different chemical compounds. Since the presence of $Cu_2CoSnS_4$ ($E_g = 1.5$ eV) was clearly identified both by XRD and Raman spectroscopy, one of the two peaks could be assigned to the quaternary chalcopyrite. Probable material candidates for the second peak could be CoS ($E_g = 0.90$ eV), $Cu_xS$ ($E_g = 1.8$–$2.4$ eV), $SnS_2$ ($E_g = 2.35$ eV), $SnO_2$ ($E_g = 3.8$ eV) or $Cu_2SnS_3$. Indeed, no experimental value is available for the quantum shift resulting from a 3 nm mean diameter $Cu_2CoSnS_4$ nanoparticle. Nevertheless, a good estimation of the quantum shift can be obtained from values previously reported for the CIS chalcopyrite displaying similar structure and optical properties. For CIS QDs, various PL peak energy ranging from 450 nm[22] (2.75 eV) to 750 nm[23] (1.65 eV) were reported for 3 nm CIS nanoparticles. From these observations, we propose that the low energy transition could be attributed to $Cu_2CoSnS_4$ QDs. Our preliminary experiments on $Cu_2FeSnS_4$ QDs have shown similar characteristics of the absorption and PL spectra demonstrating that the high energy peak do not involve Fe or Co elements, and thus suggesting that the high energy transition could be assigned to materials such as $Cu_xS$ or $SnS_2$.

Another important feature is the Stokes shift of 30–80 nm observed between the spectra recorded on the $Cu_2CoSnS_4$ QDs. Note that typical Stokes shift of 100 nm[23] and 246 meV[25] were reported in CIS QDs. For a reminder, the origin of luminescence recombination was previously attributed to donor–acceptor pair recombination in $Cu_2ZnSnS_4$ bulk single crystals[13] which possess a structure close to $Cu_2CoSnS_4$. Indeed, $Cu_2CoSnS_4$ has a complex defect chemistry because of the variation in ([Cu]/[Co] + [Sn]), [Co]/[Sn] and [S]/[Cu] ratios. Probable intrinsic defects in $Cu_2CoSnS_4$ crystals are $Cu_{Co}$, $V_{Cu}$, $Co_{Sn}$, $V_{Co}$, $Co_{Cu}$, $Sn_{Co}$,[26, 27] and excess or deficient sulfur occupancy. $Cu_2CoSnS_4$ crystals with a high concentration of defects may not exhibit band edge luminescence. Two groups of emission peaks could be observed in the literature for CIS and CZTS materials. A first group involves donor-to-valence band emission, observed in sulfur deficient crystals. It results from a recombination of an electron at a sulfur vacancy or either at a cobalt–copper substitution site with the valence band. A second group of peaks involves the recombination between donor states with acceptor states. This latter type of recombination is observed in $CuInS_2$ or $Cu_2ZnSnS_4$ samples. To better understand the transitions involved in our quantum dots, TRPL measurements were performed on films made from $Cu_2CoSnS_4$ quantum dots. Fig. 6 shows the representative PL decay curves of the $Cu_2CoSnS_4$ nanocrystals which were probed at different excitation powers. The long tail of the PL decay curve of each power excitation can be fitted by a single exponential function $I(t) = A_1\exp(-t/\tau_1)$ where $\tau_1$ represents the decay time of the PL emission and $A_1$ represents the amplitude of the decay components at $t = 0$. A short decay time $\tau_1 = 2.8$ ns was determined from the curves at room temperature. Thus shorter decay times are determined in our QDs, in contrast to values up to 300 ns, reported for $CuInS_2$ chalcopyrites nanocrystals synthesized with the use of surfactants.[25] These observations suggest that the observed PL Stokes shift does not arise from a donor–acceptor pair (DAP) recombination. Another origin of such an important PL Stokes shift can be found in the size distribution of the QDs even in the presence of intrinsic

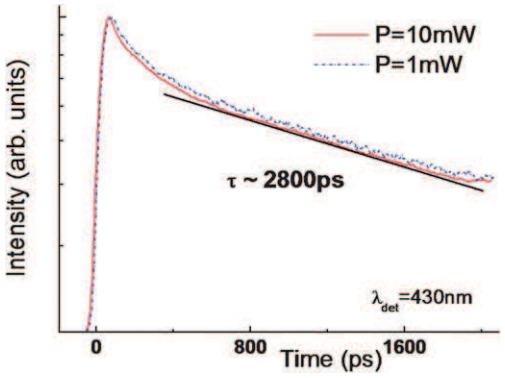


**Fig. 6** Time resolved photoluminescence intensity of $Cu_2CoSnS_4$ quantum dots showing a short decay time. Excitation $\lambda = 290$ nm, detection $\lambda = 430$ nm. $P_{aver} = 1$ and 10 mW. $T = 300$ K.

transitions as observed by Micic *et al.*[28] However, in order to precisely determine the origin of the PL emission further experimental work is needed at cryogenic temperatures.

## Conclusions

A novel process route for the synthesis of monodisperse colloidal $Cu_2CoSnS_4$ quantum dots has been developed without the use of any capping surface additive or coordinating solvent. Although a large concentration of defect exists in these nanocrystals prepared at relatively low temperature, distinct exciton peaks were clearly observed in the absorption spectra.

Corresponding PL spectra exhibited two well-defined peaks, observed at lower energies than absorption peaks. Investigations by stationary (PL) and time resolved (TRPL) photoluminescence spectroscopy demonstrate that these two peaks could not be assigned to the radiative recombination of the ground and excited state in a given size and composition QD but rather suggest transitions occurring either from two populations possessing different mean sizes or from different chemical compounds. Our observations also suggest that the observed PL Stokes shift does not arise from a donor–acceptor pair (DAP) recombination.

## Acknowledgements

We thank Alain Seraphine and Delphine Lagarde for very helpful discussions. This research was funded by Ecole des Beaux Arts et d'Architecture—Region la Reunion.

## References

1 H. X. Schock, *MRS Bull.*, 1993, **28**(10), 42.
2 M. A. Contreras, B. Egaas, K. Ramanathan, J. Hiltner, A. Swartzlander, F. Hasoon and R. Noufi, *Prog. Photovolt. Res. Appl.*, 1999, **7**, 311.
3 H. Katagiri, K. Jimbo, S. Yamada, Y. Kamimura, W. S. Maw, T. Fukano, T. Ito and T. Motohiro, *Appl. Phys. Express*, 2008, **1**, 041201.
4 T. K. Todorov, K. B. Reuter and D. B. Mitzi, *Adv. Mater.*, 2010, **22**, 1.
5 K. Ito and T. Nakazawa, *Jpn. J. Appl. Phys.*, 1988, **27**(11), 2094.
6 S. R. Hall, J. T. Szymanski and J. M. Stewart, *Can. Mineral.*, 1978, **16**, 131.
7 A. Luque and A. Marti, *Phys. Rev. Lett.*, 1997, **78**, 26.
8 H. Guillemoles, *Thin Solid Films*, 2002, **403–404**, 405.
9 R. P. Raffaelle, S. L Castro, A. F. Hepp and S. G. Bailey, *Prog. Photovolt. Res. Appl.*, 2002, **10**, 433.
10 O. Guo, H. W. Hillhouse and R. Agrawal, *J. Am. Chem. Soc.*, 2009, **131**, 11672.
11 C. Steinhagen, M. G. Panthani, V. Akhavan, B. Goodfellow, B. Koo and B. A. Korgel, *J. Am. Chem. Soc.*, 2009, **131**, 12554.
12 Y. Miyamoto, K. Tanaka, M. Oonuki, N. Moritake and H. Uchiki, *Jpn. J. Appl. Phys.*, 2008, **47**(1), 596.
13 K. Tanaka, Y. Miyamoto, H. Uchiki, K. Nakazawa and H. Araki, *Phys. Status Solidi A*, 2006, **203**(11), 2891.
14 C. Persson, *J. Appl. Phys.*, 2010, **107**(5), 053710/1.
15 Patent FR 09/04322, 2009.
16 M. Himmrich and H. Haeusler, *Spectrochim. Acta, Part A*, 1991, **47**(7), 933.
17 W. H. Koschel, F. Sorger and J. Baars, *J. Phys.*, 1975, **36**, C3–177.
18 S. Hore, E. Palomares, H. Smit, N. J. Bakker, P. Comte, P. Liska, K. R. Thampi, J. M. Kroon, A. Hinsch and J. R. Durrant, *J. Mater. Chem.*, 2005, **15**(3), 412.
19 K. Rajesh, P. Mukundan, P. K. Pillai, V. R. Nair and K. G. Warrier, *Chem. Mater.*, 2004, **16**(14), 2700.
20 C. B. Murray, D. J. Norris and M. G. Bawendi, *J. Am. Chem. Soc.*, 1993, **115**, 8706.
21 O. L. Micic, K. M. Jones, A. Cahill and A. J. Nozik, *J. Phys. Chem. B*, 1998, **102**, 9791.
22 J. J. Naim, P. J. Shapiro, B. Twamley, T. Pounds, R. Von Wandruszka, T. R. Fletcher, M. Williams, C. Wang and M. G. Norton, *Nano Lett.*, 2006, **6**(6), 1218.
23 S. L. Castro, S. G. Bailey, R. P. Raffaelle, K. K. Banger and A. F. Hepp, *J. Phys. Chem. B*, 2004, **108**, 12429.
24 J. S. Gardner, E. Shurdha, C. Wang, L. D. Lau, R. G. Rodriguez and J. J. Pak, *J. Nanopart. Res.*, 2008, **10**, 633.
25 H. Zhong, Y. Zhou, M. Ye, Y. He, J. Ye, C. He, C. Yang and Y. Li, *Chem. Mater.*, 2008, **20**, 6434.
26 V. K. Kalevich, M. Paillard, K. V. Kavokin, X. Marie, A. R. Kovsh, T. Amand, A. E. Zhukov, Y. G. Musikhim, V. M. Ustinov, E. Vanelle and B. P. Zakhachenya, *Phys. Rev. B: Condens. Matter*, 2001, **64**, 045309.
27 S. Chan, X. G. Gong, A. Walsh and S. H. Wei, *Appl. Phys.*, 2010, **96**, 021902.
28 O. I. Micic, H. M. Cheong, H. Fu, A. Zunger, J. R. Sprague, A. Mascarenhas and A. J. Nozik, *J. Phys. Chem. B*, 1997, **101**, 4904.